



ISSN: 0067-2904

Removing of Methylene Blue Dye from its Aqueous Solutions Using Polyacrylonitrile/Iron Oxide/Graphene Oxide

Yasser Yousef Muhi-Alden*, Khulood A. Saleh

Department of Chemistry, College of Science, University of Baghdad, Baghdad, Iraq

Received: 27/7/2021

Accepted: 11/10/2021

Published: 30/6/2022

Abstract

Organic contaminants are used to be found in industrial wastewater treatment procedures, and heavy metal ion removal is difficult. Photo Fenton reaction activity was exploited in this study to decompose organic contaminants using a functional composite hydrogel. Polyacrylonitrile (PAN), Fe_3O_4 particles, and graphene oxide make up the hydrogel (GO). It is made from GO/ Fe_3O_4 and is made using the precipitation technique. GO is made from graphite using the Hummers process. And it has exceptional mechanical strength and Photo-Fenton activity as a result of various breakdown data that were influenced differently, such as H_2O_2 concentration, dye concentration, temperature, and irradiation duration. Atomic Force Microscopy (AFM) was used to examine the composite's shape and average diameter. Under UV irradiation, the degradation of Methylene Blue dye (M.B) by the PAN/ Fe_3O_4 /GO hydrogel composite reached 100% after 90 min. Meanwhile, after 90 min of visible irradiation, COD (Chemical Oxygen Demand) dropped to 9 mg/L and dropped to low (sub range) after two and a half hours. This research proposes a new method for processing high-consistency industrial effluent that is difficult to decompose.

Keywords: Photo- Fenton reaction, PAN/ Fe_3O_4 /GO composite, Methylene Blue, COD.

إزالة صبغة ميثيلين الأزرق من محاليلها المائية باستخدام بولي أكريلونيتريال / أكسيد الحديد / أكسيد الجرافين

ياسر يوسف محي الدين * , خلود عبد صالح

قسم الكيمياء , كلية العلوم , جامعة بغداد , بغداد , العراق

الخلاصة

توجد الملوثات العضوية في مراحل معالجة مياه الصرف الصناعي ، ومن الصعب إزالة أيونات المعادن الثقيلة. تم استغلال نشاط تفاعل فنتون في هذه الدراسة لتحليل الملوثات العضوية باستخدام هيدروجيل مركب. تشكل مادة البولي أكريلونيتريال (PAM) وجزيئات Fe_3O_4 وأكسيد الجرافين (GO) الهيدروجيل. إنه من GO/Fe_3O_4 ويتم تحضيره باستخدام تقنية الترسيب. GO تم تحضيره من الجرافيت باستخدام عملية

*Email: YasserYousif.Muhie1205@sc.uobaghdad.edu.q

Hummers. وله قوة ميكانيكية استثنائية مع نشاط *Photo-Fenton* مما يؤدي الى تحطيم الملوثات العضوية المختلفة التي تأثرت بشكل مختلف بتركيز H_2O_2 وتركيز الصبغة ودرجة الحرارة ومدة التشعيع. تم استخدام مجهر القوة الذرية (*AFM*) لفحص شكل المركب ومتوسط قطره. تحت إشعاع الأشعة فوق البنفسجية ، وصل تدهور صبغة أزرق الميثيلين (*M.B*) بواسطة مركب $PAN/Fe_3O_4/GO$ هيدروجيل إلى 100% بعد 90 دقيقة. وفي الوقت نفسه ، بعد 90 دقيقة من التشعيع ، انخفض *COD* (الطلب على الأوكسجين الكيميائي) إلى 9 مجم / لتر وانخفض إلى المستوى المنخفض (النطاق الفرعي) بعد ساعتين ونصف. يقترح هذا البحث طريقة جديدة لمعالجة النفايات السائلة الصناعية عالية التماسك التي يصعب تحللها.

1. Introduction

Because of the ease with which wastewater may be disposed of, surface water ways are the most vulnerable to pollution[1].The Fenton reaction, which is used for wastewater treatment, includes a combination of ferrous iron (Fe^{2+}) and hydrogen peroxide (H_2O_2) in an acidic solution to form the hydroxyl radical ($\bullet OH$) [2]. Homogeneous Fenton reactions have various drawbacks, including an acidic pH, poor H_2O_2 consumption efficiency, and sludge production[3,4]. Its usefulness is limited due to these flaws. Furthermore, a high (H_2O_2) (Fe^{2+}) molar ratio necessitates a large amount of Fe^{2+} [5,6]. This increases the amount of reagents used. Solid, iron-containing compounds or solid materials rich in iron, such as Fe_3O_4 [7,8], Fe_3O_4 [9], $FeOOH$ [10], and clay [11], as well as mesoporous silica[12], are used in the heterogeneous Fenton reaction. For the breakdown of organic contaminants, iron-containing compounds were promoted. In comparison, heterogeneous Fenton reactions are an effective oxidative technology for degrading organic pollutants because they efficiently promote H_2O_2 conversion with minimal decomposition, and easy separation from solution for cyclic utilization, all of which are advantageous for practical applications. However, because of the poor contact between the iron catalyst and the carrier materials, most iron-containing catalysts are not practical and increase iron leaching after cyclic use numerous times, resulting in catalytic stability and decreased activity.[13–15] The carbon atom is one of the most abundant atoms on Earth, appearing naturally in a variety of forms and as a component in a large number of compounds known as allotropes of carbon[16].These potential characteristics have been used in a variety of applications, including electronics, batteries, sensors, and composite materials. The preparation of hydrogels with exceptional mechanical characteristics drew a large number of people.[17]. There are three common recipes for making high-strength hydrogels: topological gels [18], double network gels [19], and composite gels[20]. Composite gels are thought to improve the mechanical properties of hydrogels, for example, composite gels with a unique organic inorganic network structure would have extraordinary mechanical properties [21].

Graphene oxide (GO) is now one of the most popular study topics among chemists, owing to its inexpensive cost of mass manufacturing and excellent water dispersibility [22–24].

The chemistry of Polyacrylonitrile (PAN) is of particular importance since it is used as a matrix in the development of carbon nanofiller-based nanocomposite for different appliances. Carbon nanotubes (CNT), graphene, and graphene oxide (GO) have all been employed in bulk composite materials and thin films[25]. Recently, there has been a surge of interest in the use of composite Nanofibers NFs in water treatment, especially for the removal of organic pollutants [26-27]. Chen et al. found that calixarene-functionalized polyacrylonitrile (PAN) composite nanofibers NFs effectively adsorb Congo red[26]. Thus, photo catalytic degradation of environmental pollutants is an interesting topic for study.

2. Experimental Part

2.1 Determination of Maximum Absorption (λ_{\max}) The wavelength value of Methylene Blue dye (M.B) absorption is 650 nm, this was used to estimate its quantity as shown in Figure 1.

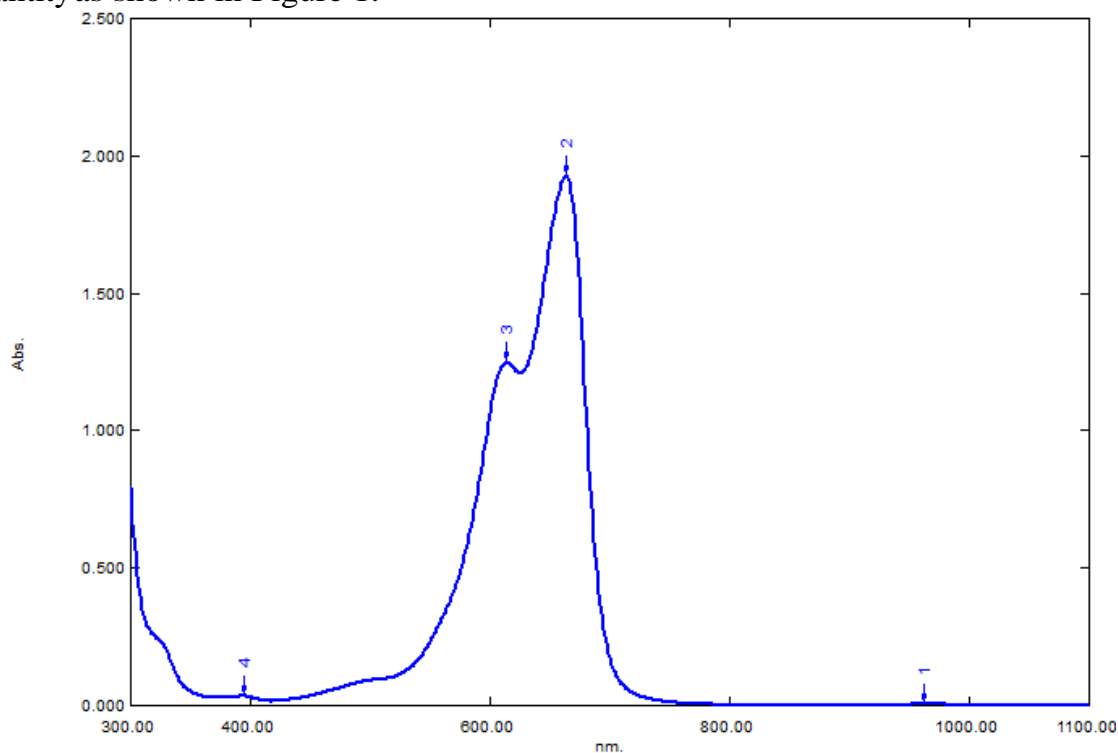


Figure 1-UV-Visible absorption spectrum for methylene blue dye

2.2 Calibration curve for M.B dye

Figure 2: illustrates the calibration curve which is the linear relation between absorbance and concentration.

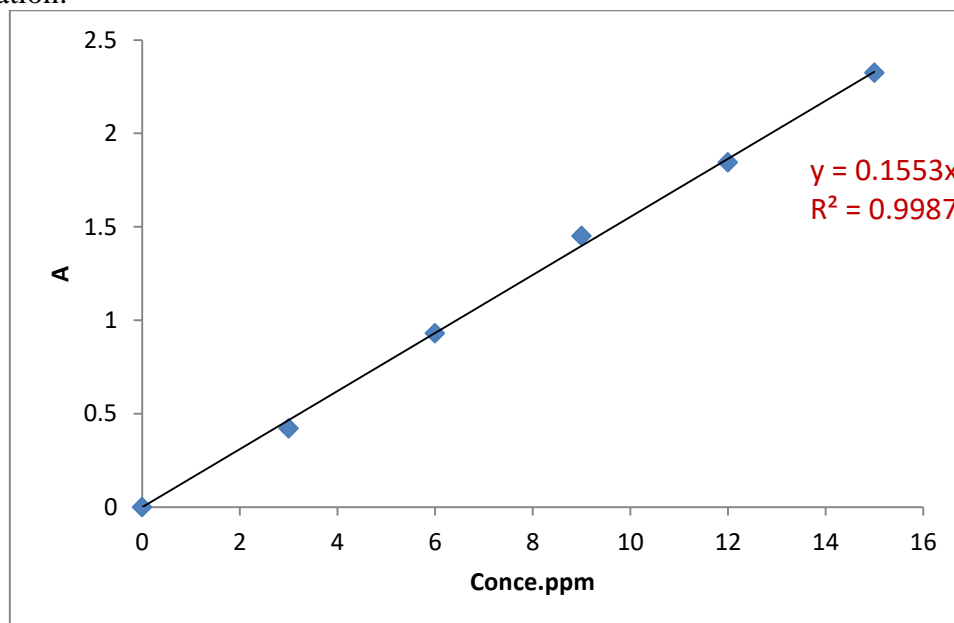


Figure 2- Calibration curve for Methylene blue

2.3 Graphene oxide (GO) preparation

Hummer's method was used to create GO from graphite [28]. 1.0 g of graphite was added into 23 ml of concentrated sulphuric acid (H_2SO_4) under stirring at room temperature, then, 0.5 g of sodium nitrate was added, and the mixture was cooled to $0^\circ C$. Under powerful agitation, 3.0 g of potassium permanganate was added slowly while the temperature of the suspension was kept near $2^\circ C$. The reaction mixture was transferred to a water bath at a temperature of $35^\circ C$ and stirred for 30 min. Then, 50 ml of deionized water (DI) was added, and the solution was stirred for 15 min at $90^\circ C$. Additional 166 ml of water was added and followed by a slow addition of 5 ml of 30% hydrogen peroxide (H_2O_2), turning the color of the solution from yellow to dark brown. The mixture was filtered and rinsed with 85 ml of 4% HCl aqueous solution which followed by washing with 65 ml of distilled water to remove the acid, then oxidation product washed until the pH reached 6, then filtered and dried. In Figure 3, FTIR spectrum of GO showed characteristic bands transmission bands of 3425, 1708, 1625, 1363, 1218, 1071 cm^{-1} belongs to stretching of (O-H) and (C=O of carbonyl groups), (C=C formative vibrations of aromatic), (C-O belong to the group of carboxylic) and epoxy and alkoxy group, respectively, this confirms the presence of successful oxidation on graphite by using the FTIR spectrum [29].

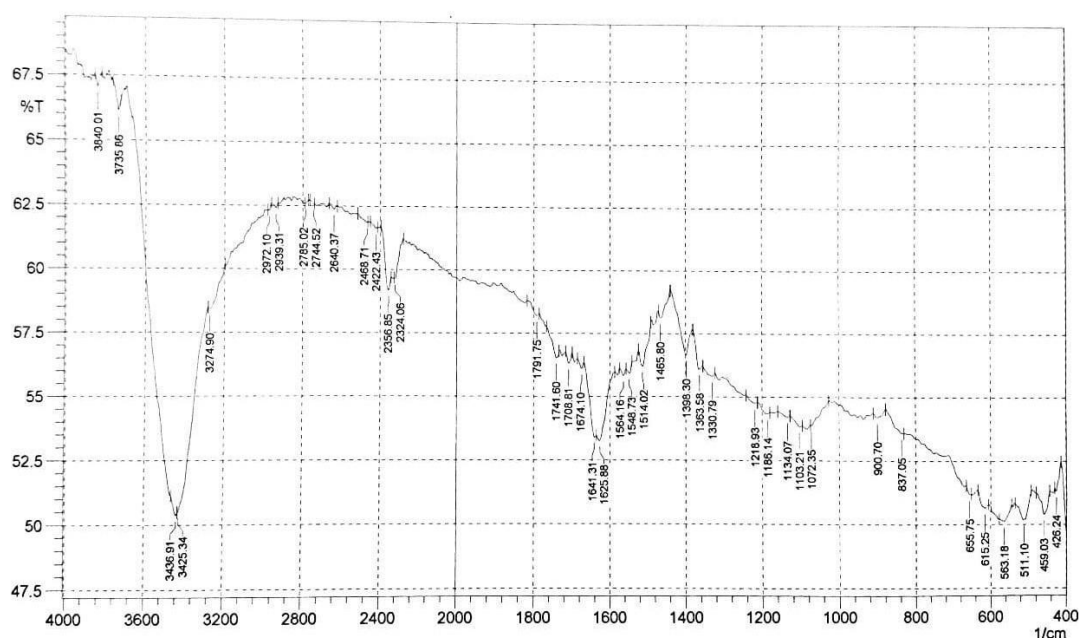


Figure 3-The FTIR spectrum of graphene oxide produced by hammers method

2.4 GO/ Fe_3O_4 composite preparation

Hummer's approach was used to make graphene oxide. To make the GO/ Fe_3O_4 composite, sonication was used to disperse 0.2 g of as-prepared graphene oxide in 150 ml of distilled water in the first stage. $FeCl_3$ and $FeCl_2$ in an aqueous solution comprising 0.140 g $FeCl_3$ and 0.0855 g $FeCl_2 \cdot 4H_2O$ was added into the graphene oxide dispersion and stirred constantly. After 2 hours of stirring, ethylamine $C_2H_5NH_2$ was dropped into the dispersion at a rate of around 1 ml per minute to precipitate Fe_3O_4 nanoparticles on the graphene oxide sheet. X-ray diagrams are shown in Figure 4 for GO/ Fe_3O_4 . XRD pattern of graphene oxide at $2\theta = 11.2408^\circ$ indicates an intercalation of water molecules and a generation of oxygenated functional groups such as epoxy and hydroxyl groups between the inner galleries of the graphite sheets during intense oxidation. For inner Fe_3O_4 , all diffraction peaks in XRD pattern, at $2\theta = 30.4917^\circ$, 35.9021° , 43.5521° , 53.945° , 57.3674° and 63.0043° can be easily indexed to the pure cubic spinel magnetite structure, which matches well with the reported

data (JCPDS: 63-3107)[30]. The peaks were intense and well defined and this indicates the optimum degree with respect to the structural arrangement in the long bands. Due to the combinations between two components, the spectrum of GO/Fe₃O₄ appears to have a partial reduction with respect to GO confirming the dispersion of ferric oxide on the graphene layers. This widening would overlap with most ferric oxide peaks due to lower concentrations of ferric oxide in the compound. This reaction took place at room temperature.

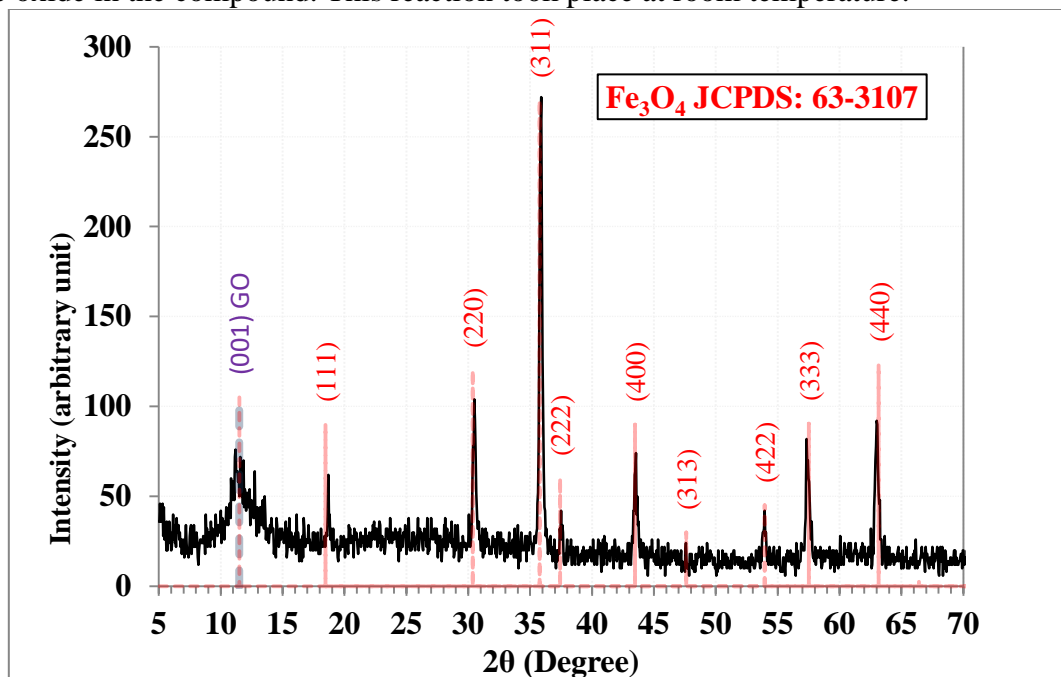


Figure 4-XRD pattern of GO/ Fe₃O₄

2.5 PAN/ Fe₃O₄/GO composite preparation

A simple solvothermal approach was used to make PAN/ Fe₃O₄/GO to make a heterogeneous solution, 0.05g of Polyacrylonitrile PAM was sonicated for 1 hour in 50 ml distill water. 1g GO/Fe₃O₄ was dissolved in the dispersion and agitated for 2 hours at room temperature. Following that, the compound was dried at room temperature for 24 hours.

2.6 Preparation of photocell

A copper coil encircled by the external cell by drop surface and coupled to them water bath was provided with a stainless steel pipe with a 1cm diameter and 15 cm length, see Figure 5. The temperature of the reactor and the lamp solution should be kept under control. The inner cellular surface was first treated with strong HF acid to make it rough and capable of capturing the casing, and then, the cell was entirely coated with PAN/Fe₃O₄/GO composite for 10 minutes to allow the production of a stable layer, and then the suspension was released from the reactor. To make the catalytic layer more stable as a coating, the photo reactor displays to 500°C in the inner reactor surface.

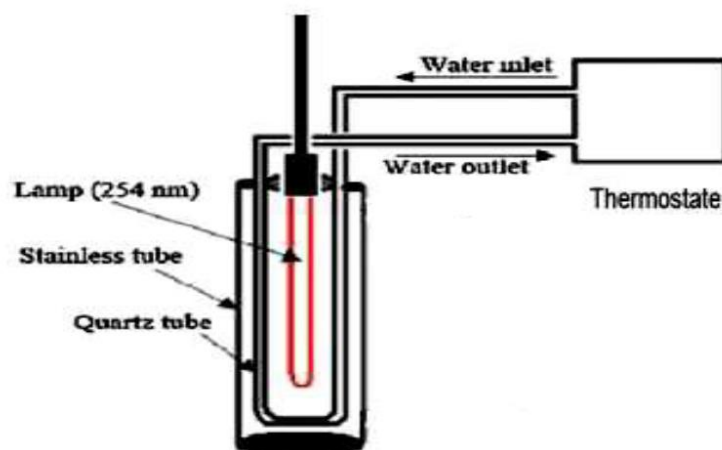


Figure 5- Complete system set up for photo degradation

3. Results and Discussion

3.1 Atomic Force Microscope (AFM)

AFM analysis provides the measurements of average grain size and the granularity cumulating distribution for GO/ Fe_3O_4 and PAN/ Fe_3O_4 /GO composites. The average diameter is 182.97 nm and 203.85 nm for GO/ Fe_3O_4 and PAN / Fe_3O_4 /GO composites, respectively. Figure 6 shows the atomic force microscopy image for: A) GO/ Fe_3O_4 composite and B) PAN/ Fe_3O_4 /GO composites.

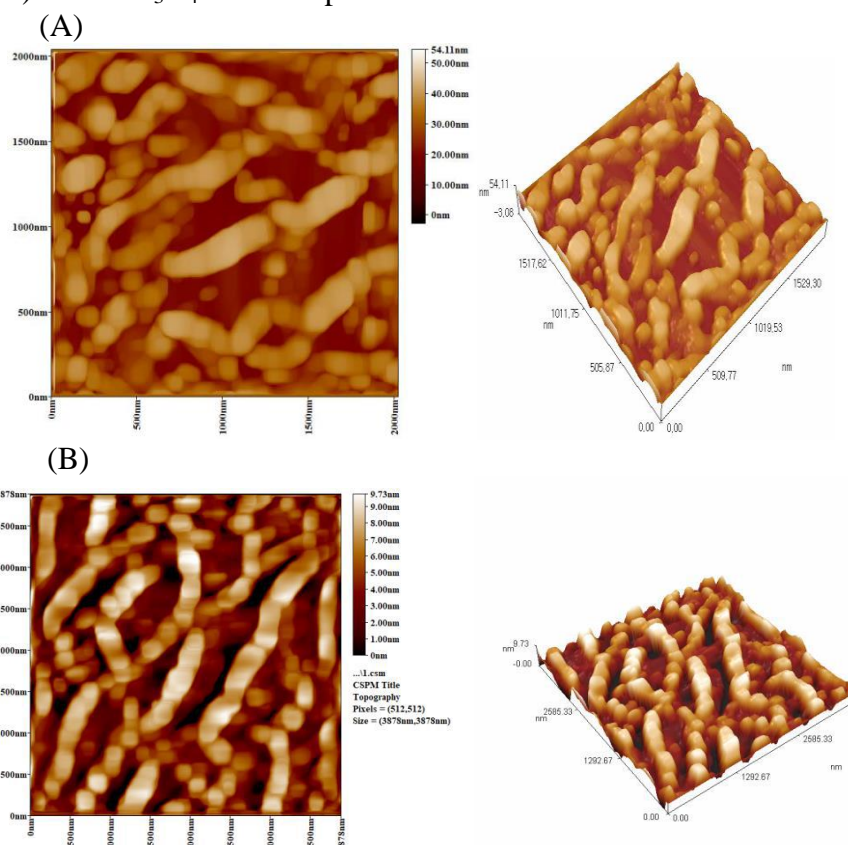


Figure 6- Atomic force microscopy image of: A) GO/ Fe_3O_4 and B) PAN/ Fe_3O_4 /GO

3.2 Effect of Initial Concentration

To study the effect of initial concentration of dye on the degradation efficiency, the experiments were conducted with different initial concentrations of (3-21) ppm at pH=7, at a temperature of 298K and 5×10^{-3} M of H_2O_2 + catalyst PAN/ Fe_3O_4 /GO composites (which

was used after 60 min). The increase of degradation percentage in each time with the decrease of M.B concentration and reach the highest value of 99.3% for 3 ppm M.B dye concentration. This phenomenon can be explained according to the indication that the number of the dye molecules will be increased with constant number regarding $\bullet\text{OH}$. Also, with the increase in dye's initial concentrations, extra molecules have been adsorbed onto catalyst's surface [31], leading to decreasing in oxidation process, as shown in Figure 7.

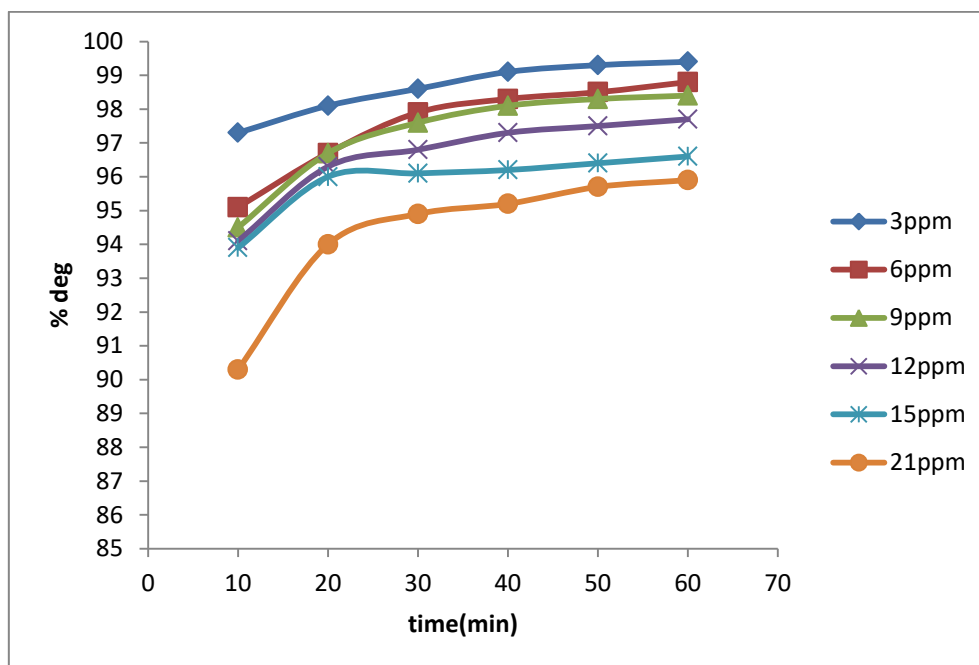


Figure 7- variation of (% deg) with time for different M.B concentration at 298K, pH=7 and H_2O_2 5×10^{-3} M by PAN/ Fe_3O_4 /GO catalyst

3.3 Effect of H_2O_2 Concentration

The effect of H_2O_2 concentration on M.B dye degradation at temperature of 289K, pH=7, after 30 min in presence of catalyst PAN/ Fe_3O_4 /GO composite were studied, the % deg increases with H_2O_2 concentration increased which is shown in Figure 8.

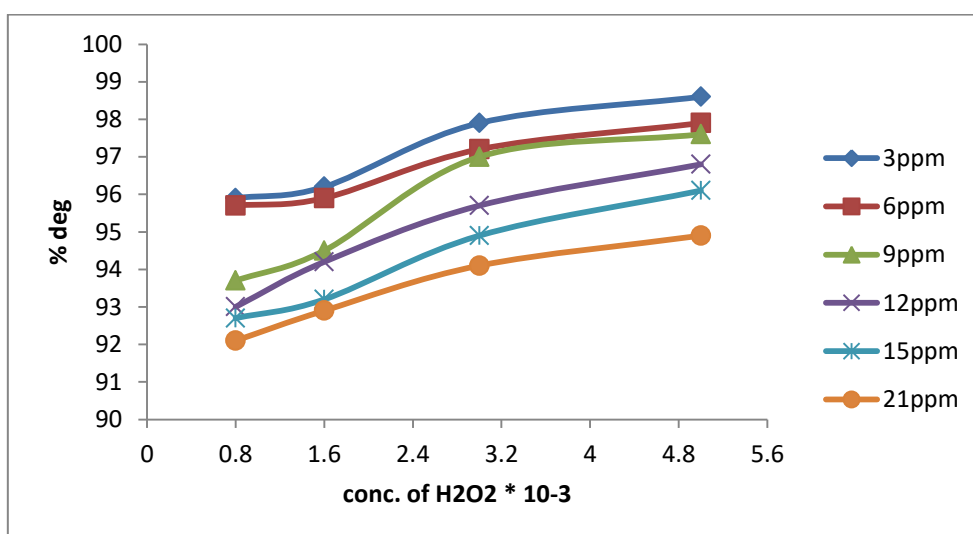


Figure 8-Effect of varying H_2O_2 concentration for different M.B concentration after 30 min, at 298K, pH=7 on PAN/ Fe_3O_4 /GO composite catalyst

3.4 Effect of Temperature

The influence of temperature on 3 ppm M.B percent deg by PAN/Fe₃O₄/GO composite at four different temperature of (298, 308, 318, and 328)K at pH=7 was examined. The deterioration of M.B increased as the temperature increased, as seen in Figure 9.

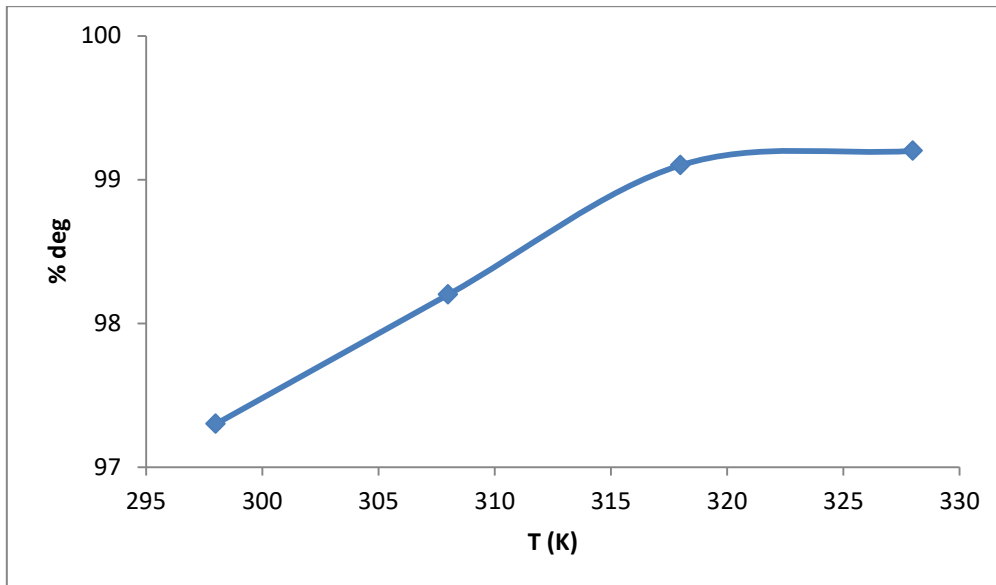


Figure 9-Variation of 3 ppm M.B %deg by PAN/ Fe₃O₄/GO composite with different temperature

3.5 Kinetic Degradation Study

Using a PAN/ Fe₃O₄/GO composite, the first order equation (1) was applied to a 3 ppm M.B degrading process with an H₂O₂ concentration of 0.005 M: When and where: C₀: initial M.B concentration, C_e: M.B concentration following UV exposure at Time(t). Figure 10 depicts the linear relation between ln C_e and time for 3 ppm M.B dye degradation at four temperatures.

$$\ln C_e = \ln C_0 - K. t \quad \dots\dots\dots(1)$$

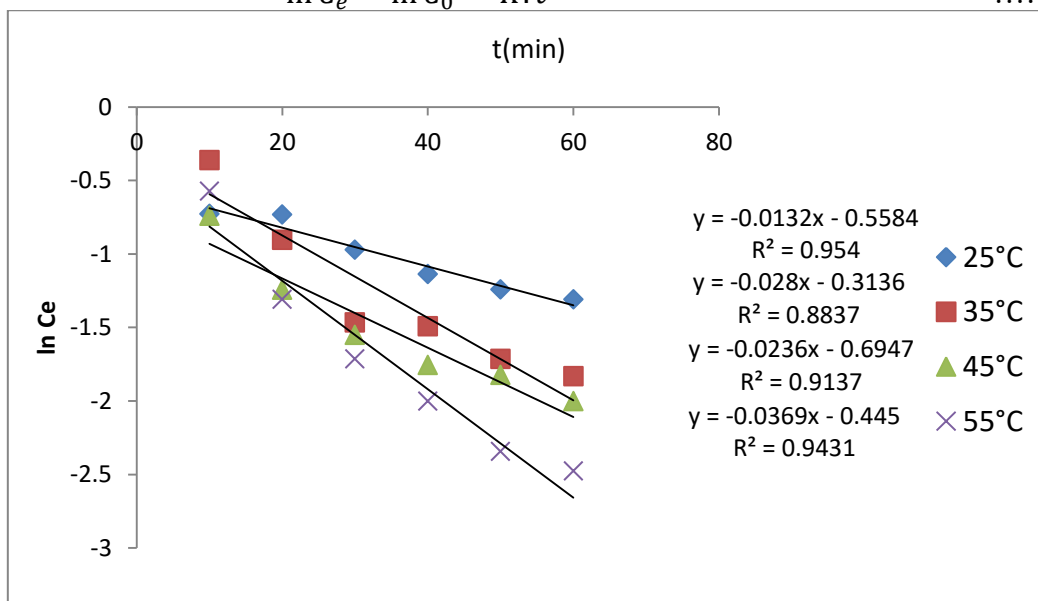


Figure-10: lnCe V.S time for the degradation of 12 ppm M.B at four temperatures by using Triple catalyst PAN/ Fe₃O₄/GO composite.

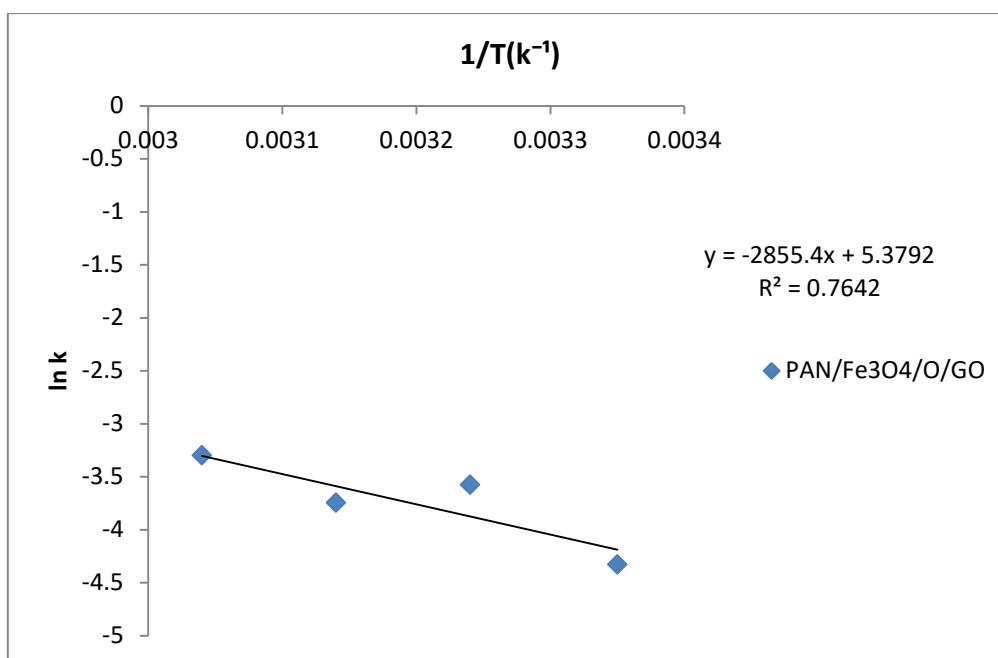


Figure 11- Arrhenius plots, relation lnk with 1/T for the 12 ppm M.B %deg. PAN/ Fe₃O₄/GO composite.

Arrhenius equation was applied to calculate kinetic parameter A, Ea. (Figure 11) as following [32]:

$$\ln k = \ln A - E_a/RT \quad \dots\dots(2)$$

Where T: is the absolute temperature (in kelvins), k is the rate constant, Ea is the reaction's activation energy (in k.J mol⁻¹), A is the pre-exponential factor, and R is the global gas constant.

The activation energy (also known as the minimum energy necessary to initiate a chemical reaction) of degradation is represented by Ea, while the pre-exponential factor in the rate equation is represented by A.

Table 1 shows the values of Ea and A obtained from the slope and intercept of the Ln k versus 1/T plot .

Table 1- Kinetic parameter for PAN/ Fe₃O₄/GO composite

	T(K)	k/(min)10 ⁻³	ln k	Ea/kJ.mol ⁻¹	A (min ⁻¹)
PAN//Fe ₃ O ₄ //GO	298	13.2	-4.32	23.739	216.8
	308	28.0	-3.57		
	318	23.6	-3.74		
	328	36.9	-3.29		

3.6 COD (Chemical Oxygen Demand) Test

COD is a commonly used as a metric method for measuring the contaminants in wastewater and natural waterways[33]. COD was eliminated by 9 mg/L of PAN/Fe₃O₄/GO composite. After 90 minutes of irradiation time for a concentration of 3 ppm M.B at pH=7, temperature 298K- and 0.005M H₂O₂. Under the same settings, after two and a half hours, this result dropped to zero.

Conclusions

In conclusion, the degradation capability of Methylene Blue dye on PAN/ Fe₃O₄/GO composite as catalysts was studied. AFM was used to characterize the composite, including its average diameter and shape. The particle size increases after adding GO/ Fe₃O₄

composite to PAN, and the percent degradation efficiency for M.B increases. Using a PAN/Fe₃O₄/GO composite as a catalyst, the Photo-Fenton method was effectively used to remove the contaminants dye. The optimum irradiation time was determined to be 90 minutes. The pH impact revealed that pH=7 had the best degradation of M.B dye on PAN/Fe₃O₄/GO composite. The degradation of M.B dyes on the PAN/Fe₃O₄/GO composite increased with increasing temperature, according to the temperature impact data. After the dye solution has been subjected to irradiation for a longer amount of time, the color has been totally eliminated and the dye has been transformed into organic material (COD test after 2h is low or under range). M.B dye degradation on PAN/Fe₃O₄/GO composite was well interpreted with the first order, according to the kinetic research findings. Finally, the utilized approach (photo Fenton procedure) is suggested for the treatment of organic compound-containing wastewater.

References

- [1] A. G. Hashim, "The physico-chemical properties of southern part of Diyala River water," *Iraqi J. Sci.*, vol. 58, no. 4C SE-Biology, pp. 2322–2331, Jan. 2018, [Online]. Available: <https://ijs.uobaghdad.edu.iq/index.php/eijs/article/view/94>.
- [2] H. J. H. Fenton, "LXXIII.—Oxidation of tartaric acid in presence of iron," *J. Chem. Soc. Trans.*, vol. 65, pp. 899–910, 1894.
- [3] M. L. Kremer, "The Fenton reaction. Dependence of the rate on pH," *J. Phys. Chem. A*, vol. 107, no. 11, pp. 1734–1741, 2003.
- [4] S. H. Lin and C. C. Lo, "Fenton process for treatment of desizing wastewater," *Water Res.*, vol. 31, no. 8, pp. 2050–2056, 1997.
- [5] B. Iurascu, I. Siminiceanu, D. Vione, M. A. Vicente, and A. Gil, "Phenol degradation in water through a heterogeneous photo-Fenton process catalyzed by Fe-treated laponite," *Water Res.*, vol. 43, no. 5, pp. 1313–1322, 2009.
- [6] K. Dercová, B. Vrana, R. Tandlich, and L. Šubová, "Fenton's type reaction and chemical pretreatment of PCBs," *Chemosphere*, vol. 39, no. 15, pp. 2621–2628, 1999.
- [7] L. Gao *et al.*, "Intrinsic peroxidase-like activity of ferromagnetic nanoparticles," *Nat. Nanotechnol.*, vol. 2, no. 9, pp. 577–583, 2007.
- [8] L. Xu and J. Wang, "Fenton-like degradation of 2, 4-dichlorophenol using Fe₃O₄ magnetic nanoparticles," *Appl. Catal. B Environ.*, vol. 123, pp. 117–126, 2012.
- [9] L. Guo, F. Chen, X. Fan, W. Cai, and J. Zhang, "S-doped α -Fe₂O₃ as a highly active heterogeneous Fenton-like catalyst towards the degradation of acid orange 7 and phenol," *Appl. Catal. B Environ.*, vol. 96, no. 1–2, pp. 162–168, 2010.
- [10] S.-S. Lin and M. D. Gurol, "Catalytic decomposition of hydrogen peroxide on iron oxide: kinetics, mechanism, and implications," *Environ. Sci. Technol.*, vol. 32, no. 10, pp. 1417–1423, 1998.
- [11] J. H. Ramirez *et al.*, "Fenton-like oxidation of Orange II solutions using heterogeneous catalysts based on saponite clay," *Appl. Catal. B Environ.*, vol. 71, no. 1–2, pp. 44–56, 2007.
- [12] J. V. Coelho *et al.*, "Effect of iron precursor on the Fenton-like activity of Fe₂O₃/mesoporous silica catalysts prepared under mild conditions," *Appl. Catal. B Environ.*, vol. 144, pp. 792–799, 2014.
- [13] R. R. Nair *et al.*, "Fine structure constant defines visual transparency of graphene," *Science* (80-.), vol. 320, no. 5881, pp. 1308, 2008.
- [14] J. Moser, A. Barreiro, and A. Bachtold, "Current-induced cleaning of graphene," *Appl. Phys. Lett.*, vol. 91, no. 16, p. 163513, 2007.
- [15] A. S. Mayorov *et al.*, "Micrometer-scale ballistic transport in encapsulated graphene at room temperature," *Nano Lett.*, vol. 11, no. 6, pp. 2396–2399, 2011.
- [16] A. K. Jeryo and Q. A. Abbas, "Synthesis of Graphene Oxide Nanoparticles by Laser Ablation System," *Iraqi J. Sci.*, vol. 61, no. 9 SE-Physics, pp. 2241–2250, Sep. 2020, doi: 10.24996/ijs.2020.61.9.11.
- [17] D. Su, M. Yao, J. Liu, Y. Zhong, X. Chen, and Z. Shao, "Enhancing mechanical properties of silk fibroin hydrogel through restricting the growth of β -sheet domains," *ACS Appl. Mater. Interfaces*,

- vol. 9, no. 20, pp. 17489–17498, 2017.
- [18] Y. Okumura and K. Ito, “The polyrotaxane gel: A topological gel by figure-of-eight cross-links,” *Adv. Mater.*, vol. 13, no. 7, pp. 485–487, 2001.
- [19] J. P. Gong, “Why are double network hydrogels so tough?,” *Soft Matter*, vol. 6, no. 12, pp. 2583–2590, 2010.
- [20] K. Haraguchi and T. Takehisa, “Nanocomposite hydrogels: A unique organic–inorganic network structure with extraordinary mechanical, optical, and swelling/de-swelling properties,” *Adv. Mater.*, vol. 14, no. 16, pp. 1120–1124, 2002.
- [21] W. L. Hom and S. R. Bhatia, “Significant enhancement of elasticity in alginate-clay nanocomposite hydrogels with PEO-PPO-PEO copolymers,” *Polymer (Guildf.)*, vol. 109, pp. 170–175, 2017.
- [22] M. Xing, F. Shen, B. Qiu, and J. Zhang, “Highly-dispersed boron-doped graphene nanosheets loaded with TiO₂ nanoparticles for enhancing CO₂ photoreduction,” *Sci. Rep.*, vol. 4, no. 1, pp. 1–7, 2014.
- [23] B. Qiu, M. Xing, and J. Zhang, “Stöber-like method to synthesize ultralight, porous, stretchable Fe₂O₃/graphene aerogels for excellent performance in photo-Fenton reaction and electrochemical capacitors,” *J. Mater. Chem. A*, vol. 3, no. 24, pp. 12820–12827, 2015.
- [24] B. Qiu, M. Xing, and J. Zhang, “Mesoporous TiO₂ nanocrystals grown in situ on graphene aerogels for high photocatalysis and lithium-ion batteries,” *J. Am. Chem. Soc.*, vol. 136, no. 16, pp. 5852–5855, 2014.
- [25] A. Kausar and S. Anwar, “Graphite filler-based nanocomposites with thermoplastic polymers: a review,” *Polym. Plast. Technol. Eng.*, vol. 57, no. 6, pp. 565–580, 2018.
- [26] M. Chen *et al.*, “Electrospinning of calixarene-functionalized polyacrylonitrile nanofiber membranes and application as an adsorbent and catalyst support,” *Langmuir*, vol. 29, no. 38, pp. 11858–11867, 2013.
- [27] M. Teng, J. Qiao, F. Li, and P. K. Bera, “Electrospun mesoporous carbon nanofibers produced from phenolic resin and their use in the adsorption of large dye molecules,” *Carbon N. Y.*, vol. 50, no. 8, pp. 2877–2886, 2012.
- [28] S. William, J. R. Hummers, and R. E. Offeman, “Preparation of graphitic oxide,” *J. Am. Chem. Soc.*, vol. 80, no. 6, pp. 1339, 1958.
- [29] D. C. Marcano *et al.*, “Improved synthesis of graphene oxide,” *ACS Nano*, vol. 4, no. 8, pp. 4806–4814, 2010.
- [30] R. Hatel, S. El Majdoub, A. Bakour, M. Khenfouch, and M. Baitoul, “Graphene oxide/Fe₃O₄ nanorods composite: structural and Raman investigation,” in *Journal of Physics: Conference Series*, 2018, vol. 1081, no. 1, pp. 12006.
- [31] F. M. D. Chequer, G. A. R. De Oliveira, E. R. A. Ferraz, J. C. Cardoso, M. V. B. Zanoni, and D. P. de Oliveira, “Textile dyes: dyeing process and environmental impact,” *Eco-friendly Text. Dye. Finish.*, vol. 6, no. 6, pp. 151–176, 2013.
- [32] S. Arrhenius, “Über die Dissociationswärme und den Einfluss der Temperatur auf den Dissociationsgrad der Elektrolyte,” *Zeitschrift für Phys. Chemie*, vol. 4, no. 1, pp. 96–116, 1889.
- [33] V. Kavitha and K. Palanivelu, “Destruction of cresols by Fenton oxidation process,” *Water Res.*, vol. 39, no. 13, pp. 3062–3072, 2005.